Abstract

Adult neurogenesis is the process of generating functional neurons from neural stem cells (NSCs) in the adult brain. In humans, this unique form of neuroplasticity is restricted to the dentate gyrus (DG) of the hippocampus. Unlike developmental neurogenesis, adult neurogenesis is regulated by local and long distance neuronal circuit activity. However, the identities of specific cell types, neurotransmitters, and receptors that facilitate this regulation remain largely unknown. Studies utilizing animal and cell culture models suggest that the neuropeptide cholecystokinin (CCK) serves as a mitogenic signal for NSCs in the adult brain, but the direct effects of CCK have remained unclear. We therefore tested the hypothesis that CCK regulates adult neurogenesis by promoting NSC proliferation. We have found that NSCs express mRNA encoding the G_q-coupled CCK_2 receptor. These receptors were found to be functional after exhibiting calcium activity following stimulation with the CCK_2-receptor selective form of CCK (CCK_8). This latter effect can be blocked by the CCK_2 receptor antagonist YM022. *In-vivo* chemogenetic stimulation of CCK-releasing cells in the DG produced an increase in NSC proliferation. However, this increase in NSC proliferation did not result in an increase in total NSC density, which suggests that CCK promotes NSCs to proliferate asymmetrically rather than self-renew. In addition, shRNA-mediated knockdown of CCK8 in the DG produced a striking decrease in NSC proliferation. This information could contribute to facilitating the regeneration of neurons after brain injury and assist future treatment programs for neurodegenerative diseases.

1. Introduction

The discovery of adult neurogenesis has rewritten much of the canonical dogma of neuroscience; "nerve paths are something fixed, ended, and immutable; everything may die, nothing may be regenerated[1]" no longer holds true. However, the mechanisms that govern the generation of new neurons and their integration into existing neural circuitry are poorly understood. What is known is that dynamic neural activity regulates the generation of new neurons and their functional integration into existing circuitry. However, the exact neurotransmitter systems and receptors that regulate adult neurogenesis remain to be fully elucidated.

Neurogenesis was originally thought to occur solely during the embryonic and early postnatal stages of mammalian central nervous system (CNS) development[2]. Only recently has it become widely accepted that neurogenesis occurs throughout life, though in restricted regions of the brain. In humans, this process is limited to the subgranular zone (SGZ) of the dentate gyrus (DG) in the hippocampus[3,4,5]—a brain region critical for memory processes and affective state regulation.

Adult hippocampal neurogenesis recapitulates much of the neuronal developmental process in the mature CNS: proliferation and fate specification of adult neural precursors, morphogenesis, migration, axonal and dendritic development, and finally, synapse formation[6,7]. Neuronal development culminates in the full integration of new neurons into the existing circuitry, as depicted in Figure 1.

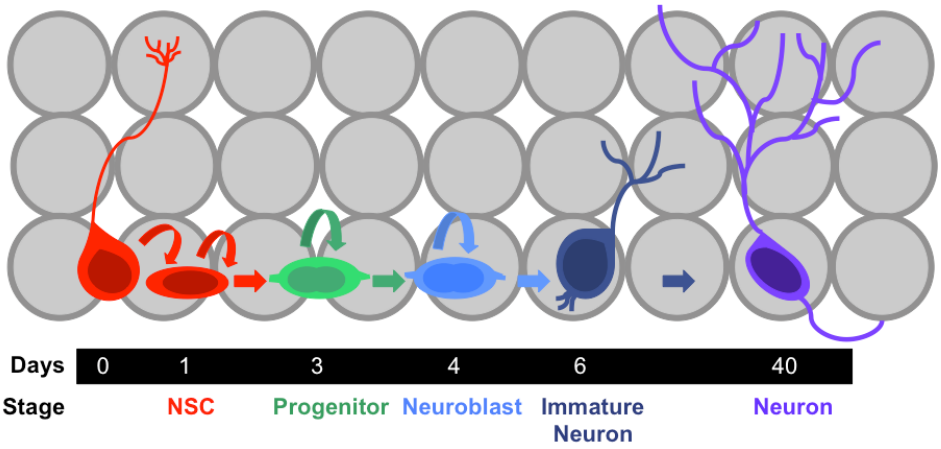

Figure 1. Illustration of the five developmental stages during adult hippocampal neurogenesis. Local neuronal activity and afferent inputs play a role in regulating whether these cells differentiate or self-renew.

However, unlike developmental neurogenesis, adult neurogenesis is finely tuned to changes in local and afferent neuronal activity (Figure 2). Currently unknown neuronal systems and pathways relay these changes in activity to NSCs. The lack of knowledge regarding the mechanisms by which different signaling systems regulate adult neurogenesis has limited the ability to manipulate the neurogenesis process to determine its specific contribution to brain functions. Thus, there is a pressing need for basic science research to understand the fundamental mechanisms involved in this process before any significant progress can be made towards translational research on adult neurogenesis.

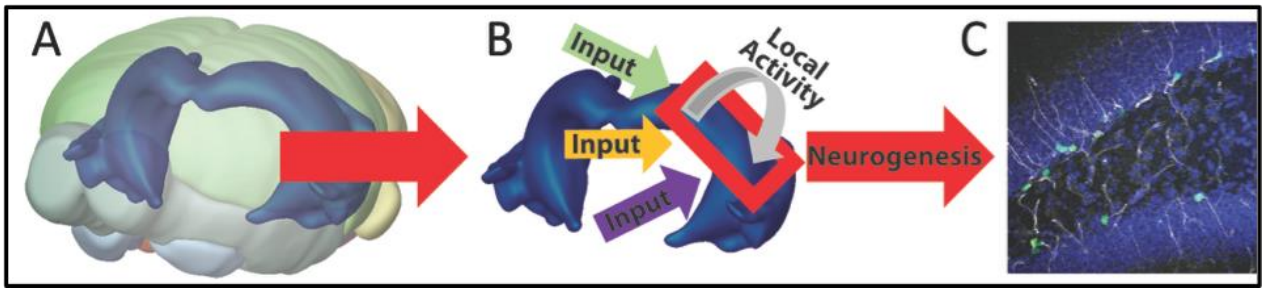

Figure 2. Model of neurogenesis regulation by neuronal activity. **(A)** Location of the hippocampus in the mouse brain. **(B)** Neuronal inputs to the hippocampus and from local neurons mediate the dynamics of neurogenesis. **(C)** Proliferating NSCs in the adult hippocampus (Green = proliferation marker; Blue = nuclear counterstain showing all cell nuclei; White radial process = stem cell marker, Nestin).

Cholecystokinin (CCK) has been identified as one of the most abundant peptides found in the brain[8]. Although CCK was originally found in the gastrointestinal tract, one of its molecular forms, cholecystokinin sulfated octapeptide (CCK8), has been discovered in high levels in the hippocampus[8]. CCK acts through two classes of G-protein coupled receptors. CCK_2 receptors represent the predominant subtype in the brain while CCK_1 receptors are mainly found in the gut[8,9]. Studies have demonstrated that CCK8 binds to CCK_2 receptors with great affinity, and has been implicated in mediating memory processes[9,10,11]. CCK8 levels and CCK_2 receptors have been found to dramatically decrease in the brain with age[11]. This effect suggests that CCK8 neurotransmission may play a role in memory impairment found in the aged.

The molecular mechanisms by which CCK is involved in the adult neurogenesis process are currently being studied. Previous studies have shown that CCK promotes the proliferation and survival of cultured neuroblasts[12] and that CCK_2 receptor knock-out mice exhibit reduced adult neurogenesis[13]. In addition, CCK promotes dendritic development *in-vitro,* which can be blocked by co-incubation with a CCK_2 receptor antagonist[14]. Such studies utilizing animal and cell culture models have suggested that CCK serves as a mitogenic signal for NSCs in the adult brain, but the molecular mechanisms and cellular targets underlying the effects of CCK remain unclear. We hypothesize that CCK regulates adult neurogenesis by promoting NSC proliferation *in-vivo*. Identifying the specific components of the CCK-cell system is a primary focus of this ongoing project.

2. Methods

2.1: Mice breeding

For the following experiments, two orthologous mouse lines were bred in the rodent animal care facility of the Genetic Medical Building at the University of North Carolina. Mice

expressing the cre-recombinase enzyme under the CCK promoter were used in Sections 2.2-2.6. VGLUT3-Cre mice were used in Section 2.7. Animals were exposed to an alternating 14-hour light and 10-hour dark cycle with free access to food and water. All mice handling and experiments were conducted in accordance with the National Institute of Health guidelines and were approved by the Institutional Animal Care and Use Committee of the University of North Carolina.

2.2: CCK localization

A cre-dependent adeno-associated virus (AAV) conjugated to the fluorescent reporter mCherry (AAV-DIO-mCherry) was delivered into the DG of 8-week old CCK-Cre mice by stereotaxic surgery. The following coordinates (in mm) were used to perform the injection: AP: -2.0; ML: 1.5; DV: -2.3 from bregma. A Hamilton syringe was used to inject 0.3 µl of the virus bilaterally at a rate of 0.1 µl per minute. Mice were given 4 weeks to recover after surgery. Following recovery, animals were injected with a lethal dose of a ketamine cocktail (40 mg/kg ketamine; 40 mg/mL xylazine) and were then transcardially perfused using 0.1M PBS (pH 7.4) followed by 4% paraformaldehyde at 4°C. Coronal brain slices (40 µm) of the entire hippocampus were collected in serial order using a Leica SM2010 R microtome.

2.3: CCK_2 receptor in-situ hybridization

Primer Blast was used to design primers to amplify a 1 kB fragment of the CCK_2 gene by the polymerase chain reaction. The following forward and reverse primers were used, respectively: 5'-ATTTAAGAGCAGTCACCCTCCCG-3' and 5'-TGAGGGGCAGAAGGAAATCTCTTTAATAGC-3'. The insert sequence was ligated into a pGEM-4Z plasmid vector containing the promoters for the DNA-dependent SP6 and T7 RNA polymerases. The plasmid containing the anti-sense probe was linearized by digestion using the

EcoRI restriction enzyme. The anti-sense probe was generated using the T7 polymerase. Digoxigenin-11-*UTP* was incorporated into the probe to allow for visualization. Frozen sections of the hippocampus (40 μm) were harvested and mounted on RNase free slides. All hybridization steps and washes followed that of a previously established protocol[15]. Visualization of Digoxigenin-11-*UTP* labeled RNA probes was achieved by TSA amplification[15].

2.4: Calcium imaging

A CCK-Cre mouse was anaesthetized by ketamine overdose and perfused with cutting buffer (in mM: 110.0 choline chloride, 2.5 KCl, 1.3 NaH_2PO_4, 25.0 $NaHCO_3$, 0.5 $CaCl_2.2H_2O$, 7.0 $MgSO_4$, 20.0 D-glucose, 1.3 sodium L-ascorbate, 3.0 sodium pyruvate, 5.5 kynurenic acid). The brain was quickly placed in ice-cold cutting buffer solution. Slices (300 μm) were sectioned using a vibratome (Leica VT1000S) and transferred to a chamber containing artificial cerebrospinal fluid (in mM: 125.0 NaCl, 2.5 KCl, 1.3 KH_2PO_4, 1.3 $MgSO_4$, 25.0 $NaHCO_3$, 2.0 $CaCl_2.2H_2O$, 1.3 sodium L-ascorbate, 0.6 sodium pyruvate, 10.0 D-glucose, pH 7.4, 32ºC), bubbled with 95% O_2/5% CO_2. A bolus-loading protocol[16] was followed where SR101 (1 uM) was added in the calcium indicator dye (Oregon Green 488 BAPTA-1, Invitrogen) to label hippocampal NSCs. Intracellular calcium change was measured by change in fluorescence. For each cell (n=4), baseline NSC activity was recorded for 30 seconds using a confocal microscope. CCK8 (500 nM) was applied to the slices through the perfusion system[16] from 30 seconds to 120 seconds while NSC activity continued to be recorded. CCK8 was then removed from the system, and fluorescence continued to be recorded for an additional 90 seconds. A fresh slice was taken, and for each cell recorded (n=4), its baseline NSC activity was recorded for 30 seconds. The slice was then pre-incubated with the CCK_2-selective antagonist YM022 (2 μm) for 30 seconds. CCK8 was subsequently applied to the slice from 30 seconds to 120 seconds, and

fluorescence was recorded over time. YM022 and CCK8 were removed from the system, and fluorescence was again measured for an additional 90 seconds.

2.5: Chemogenetic activation of CCK-cells

Utilizing cre-dependent AAV, we selectively infected and expressed the chemogenetic tool, "Designer Receptors Exclusively Activated by Designer Drugs" (DREADDs), in CCK releasing interneurons (CCK-cells) of the DG. An excitatory DREADD packaged in an AAV (AAV-DIO-h3MD-mCherry) was used to increase the activity in CCK-cells. Stereotaxic surgery was used to bilaterally inject the virus (0.3 µl) directly into the DG of 8-week old CCK-Cre experimental mice (n=5) at the following coordinates: AP: -2.0; ML: 1.5; DV: -2.3 from bregma. A fluorescently tagged control virus (AAV-DIO-mCherry) was similarly injected into the DG of 8-week old CCK-Cre control mice (n=3). Mice were given 4 weeks to recover. Clozapine-N-Oxide (CNO) administered through the drinking water (0.25 mg/mL) was given to the mice to activate the cre-dependent DREADD construct. Following 4 days of DREADD-induced activation of CCK-cells, the DNA (thymidine) analogue EdU (4 mg/kg, every 2 hours, for 4 times) was injected to label proliferating cells. Animals were transcardially perfused with 0.1M PBS (pH 7.4) followed by 4% paraformaldehyde at 4°C to preserve the tissue for histology. Coronal brain slices of the hippocampus (40 µm) were taken in serial order.

2.6.1: Construction of AAV-CCK-shRNA

CCK synthesis was disrupted using an AAV-expressing shRNA targeted to CCK. A 15 base pair sequence in the coding region of the CCK gene (5'-GAACTCGCCAAGCCAGCTGATTTC-3') was identified as the target region[17]. CCK-shRNA was designed using previously published criteria[17]. A negative control virus was similarly created using a previously identified scrambled RNA sequence

(5'-CGGAATTTAGTTACGGGGATCCAC-3') that had no known sequence similarities[17].

2.6.2: Western blot

A western blot was performed to determine the effectiveness of AAV-mediated knockdown of CCK. CCK-Cre mice (n=4) stereotaxically received three injections of CCK-shRNA at 1 uL each at the following coordinates (in mm): AP: -2.0; ML: 1.5; DV: -2.3, -2.1, -1.15 from bregma. Scramble-shRNA (1 uL) was similarly injected into the DG of the CCK-Cre control mice (n=3). After 4 weeks, mice were anaesthetized by ketamine overdose and transcardially perfused as previously described. The hippocampus was acutely dissected out from the whole brain and flash frozen in liquid nitrogen. Lysate was prepared from the tissue[16], and a western blot was performed using standard procedures with anti-CCK8 (rabbit, 1:1000 dilution) and anti-GAPDH (Abcam, rabbit, 1:1000 dilution) antibodies. Signal was detected using an Odyssey Imager (LI-COR Biosciences). Analysis utilized ImageJ to measure densitometry as a ratio of CCK8 to GAPDH total protein expression.

2.6.3: Chemogenetic activation of CCK-cells following CCK knockdown

CCK-Cre mice were given three injections of either CCK-shRNA (n=4) or scramble-shRNA (n=3) as described above in Section 2.6.2, and were given 4 weeks to recover. Following recovery, stereotaxic surgery was used to bilaterally inject the excitatory DREADD (AAV-DIO-h3MD-mCherry) directly into the DG of both groups of mice as described above in Section 2.5. Mice were given 4 weeks to recover. CNO was administered through the drinking water (0.25 mg/mL) to activate the DREADD construct. Following 4 days of DREADD-induced activation of CCK-cells, EdU (4 mg/kg, every 2 hours, for 4 times) was injected to label proliferating cells. Animals were transcardially perfused with 0.1M PBS (pH 7.4) followed by

4% paraformaldehyde at 4°C. Coronal brain slices of the hippocampus (40 µm) were taken in serial order.

2.7: Chemogenetic activation of VGLUT3-expressing CCK-cells

At 8 weeks, injection methods described above in Section 2.5 were repeated where VGLUT3-Cre experimental mice (n=4) were injected with AAV-DIO-h3MD-mCherry. VGLUT3-Cre control mice (n=4) were injected with AAV-DIO-mCherry. The mice were given 4 weeks to recover and were then administered CNO (0.25 mg/mL) through the drinking water for 4 days. Animals were subsequently perfused as described previously. Coronal brain slices of the hippocampus (40 µm) were taken in serial order.

2.8: Immunohistochemistry, confocal imaging, and quantification

To visualize the localization of the virus in Section 2.2, immunostaining was performed with the following antibodies: anti-mCherry (Abcam, mouse, 1:250 dilution) to label CCK-cells, anti-CCK8 (rabbit, 1:250 dilution) to label CCK8, and anti-GFAP (Abcam, chicken, 1:250 dilution) to label NSCs. DAPI (4',6-diamidino-2-phenylindole) (Invitrogen, 1:125 dilution) was used to label cell nuclei. Tissue from Section 2.3 was stained with anti-GFAP (Abcam, chicken, 1:250 dilution) and DAPI (Invitrogen, 1:125 dilution). In Sections 2.5 and 2.6.3, immunostaining was performed on every seventh brain section of the hippocampus. An antigen retrieval protocol[18] was performed by microwaving sections in boiling citric buffer for 7 minutes. EdU labeling[19] was completed using either Life Technologies Alexa Fluor 488 azide (for Section 2.5) or Alexa Fluor 594 azide (for Section 2.6.3). Anti-Nestin (Aves, chicken, 1:250 dilution) was used to label NSCs. For Section 2.7, the following antibodies were used: anti-Nestin (Aves, chicken, 1:250 dilution) and anti-MCM2 (Abcam, rabbit, 1:250 dilution).

Images were acquired on an Olympus Fluoview FV1000 confocal microscope with a 40X objective lens using multitrack configuration. To analyze the proliferation of NSCs, the incorporation of the proliferation marker into $Nestin^+$ NSCs was quantified. To analyze the total proliferation in the DG, all cells that incorporated the proliferation marker were quantified. To analyze the total NSCs located in the DG, all $Nestin^+$ cells were quantified. Densitometry measurements were taken using ImageJ. The experimental group in each experiment were compared to their respective control group. All analyses were performed by investigators blind to experimental conditions. Statistical analyses were performed using Student's *t*-test.

3. Results

3.1: CCK localization

Immunohistochemistry was used to locate CCK-cells in the DG. Images revealed that CCK-cells were localized in the SGZ of the hippocampus (Figure 3A-B, 3F-G). Verification of the somatic targeting patterns of CCK-cells was confirmed by immunohistochemistry against CCK8 (Figure 3C, 3H). Staining revealed that local CCK-cell projections ramify the NSC rich region of the DG (Figure 3E).

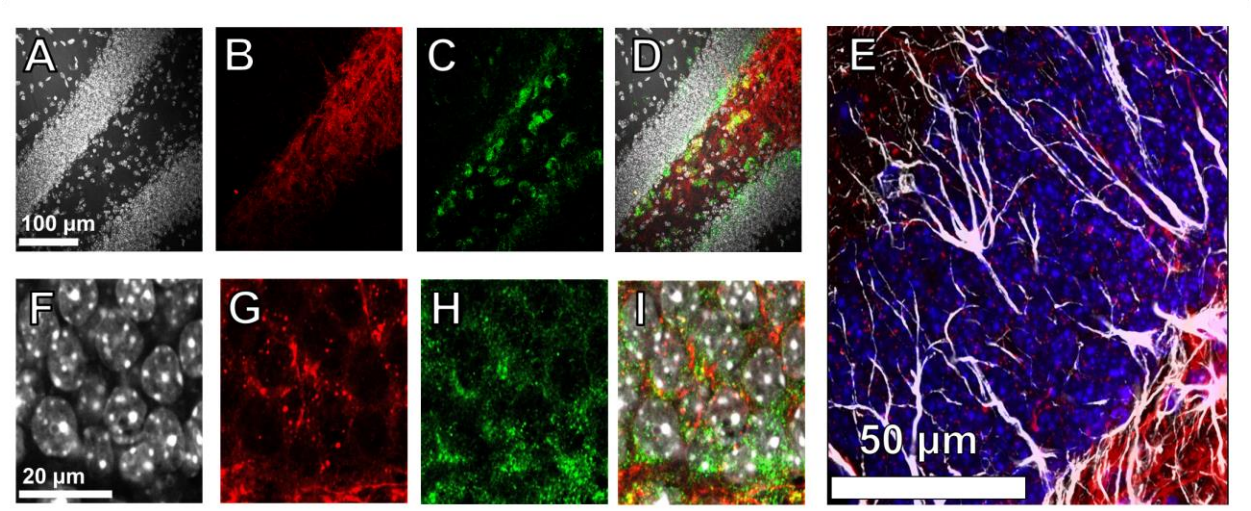

Figure 3. (A-C): Single-channel Z-stack images of the mouse DG (gray = DAPI). CCK-cells were labeled with mCherry (red) through stereotaxic delivery of a cre-dependent AAV-virus in CCK-Cre mice. Specific targeting of CCK-cells was confirmed by immunohistochemistry against CCK8 (green). **(D)** Composite overlay of images from A-C. **(E)** mCherry-labeled CCK fibers (red) densely innervated the soma of DG cells (blue) immediately proximal to radial processes (white) coming from the SGZ. **(F-H)** Single-channel high-resolution confocal images of somatic targeting patterns of mCherry labeled CCK-cells (red) co-stained for CCK8 (green) in the subgranular and granular zone of the DG (gray=DAPI). **(I)** Composite overlay of images from F-H.

3.2: In-situ hybridization

In-situ hybridization was used to determine whether NSCs possess CCK_2 receptor mRNA. Probes were correctly synthesized as shown by the colocalization of the CCK_2 probe and $GFAP^+$ NSCs (Figure 4). These images revealed that NSCs in the DG express CCK_2 receptors.

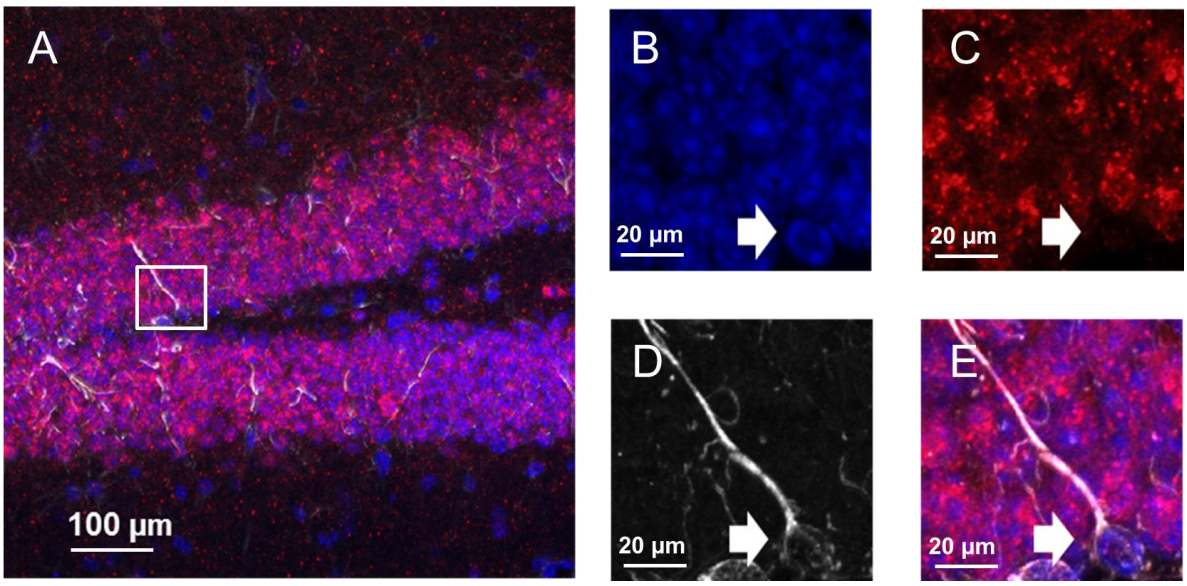

Figure 4. (A) CCK_2 receptor mRNA probes (red) localized in the mouse hippocampus. **(B-D)** Single-channel Z stack images of cell nuclei labeled with DAPI (blue), CCK_2 mRNA (red) colocalizing to $GFAP^+$ labeled NSC (white). **(E)** Composite overlay of images B-D.

3.3: Calcium imaging

To investigate whether the CCK_2 receptors identified on NSCs were functional, calcium imaging was used to test how these receptors responded to the presence of CCK8. Intracellular calcium change, represented by change in fluorescence, was measured over time. Following induction with CCK8 (500 nM), SR101-labeled NSCs exhibited a significant increase in average intracellular calcium response (25.81% ± 6.674, p=0.0306; Figure 5A) in comparison to its baseline. Additionally, it was found that the CCK8-induced calcium response could be blocked by pre-incubation with the CCK_2-selective antagonist YM022, as demonstrated by the lack of significant fluorescence change (-3.136% ± 2.513, p=0.3006; Figure 5B). These results reveal that hippocampal NSCs likely express functional CCK_2-receptors.

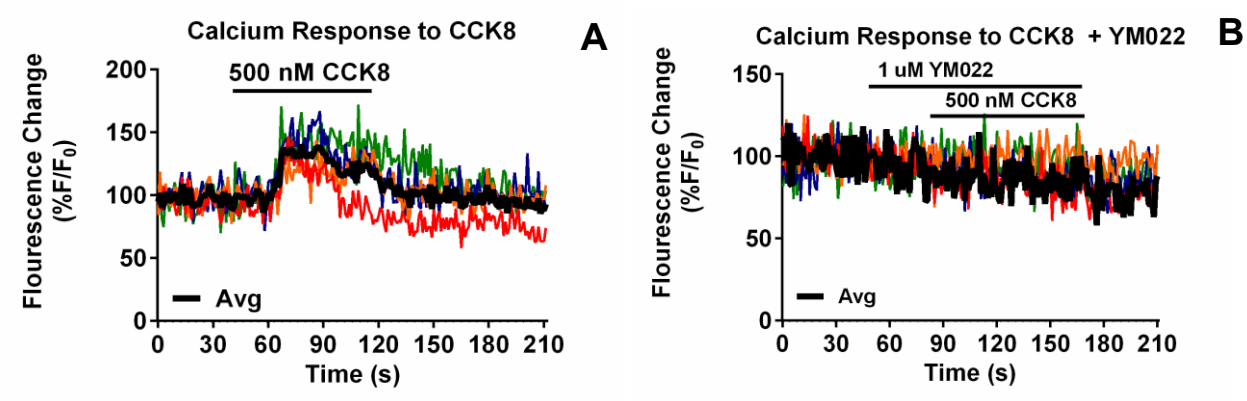

Figure 5. (A) Application of CCK8 produced an increase in intracellular calcium release in SR101-labeled NSCs (n=4) as a result of CCK_2-receptor activation. **(B)** This effect was blocked by the application of the CCK_2-antagonist YMO22 in NSCs (n=4).

3.4: Chemogenetic activation of CCK-cells

To quantify the effects of DREADD activation of CCK-cells, we measured the percentage of proliferating NSCs (number of proliferating NSCs/total number of NSCs), the density of NSC proliferation (number of proliferating NSCs/volume of DG), the total proliferation density (number of proliferating cells/volume of DG), and the total NSC density (number of NSCs/volume of DG) in both the experimental and control groups. CCK-cell activation significantly increased the percentage of proliferating NSCs in comparison to the control group, in which mice were subjected to AAV-DIO-mCherry injections, and therefore, did not have their CCK-cells activated upon CNO administration (6.709 ± 0.4001 vs. 4.489 ± 0.07500, p=0.0061; Figure 6A). In addition to an increase in the percentage of proliferating NSCs, CCK-cell stimulation significantly increased the density of proliferating NSCs (2833 ± 203.6 vs. 1859 ± 297.4, p=0.0311; Figure 6B) as well as the total proliferation in the DG (19303 ± 2326 vs. 11732 ± 1734, p=0.0645; Figure 6C). However, CCK-cell activation did not result in a significant change in the total NSC density (42776 ± 3871 vs. 41595 ± 7041, p=0.8766; Figure 6D).

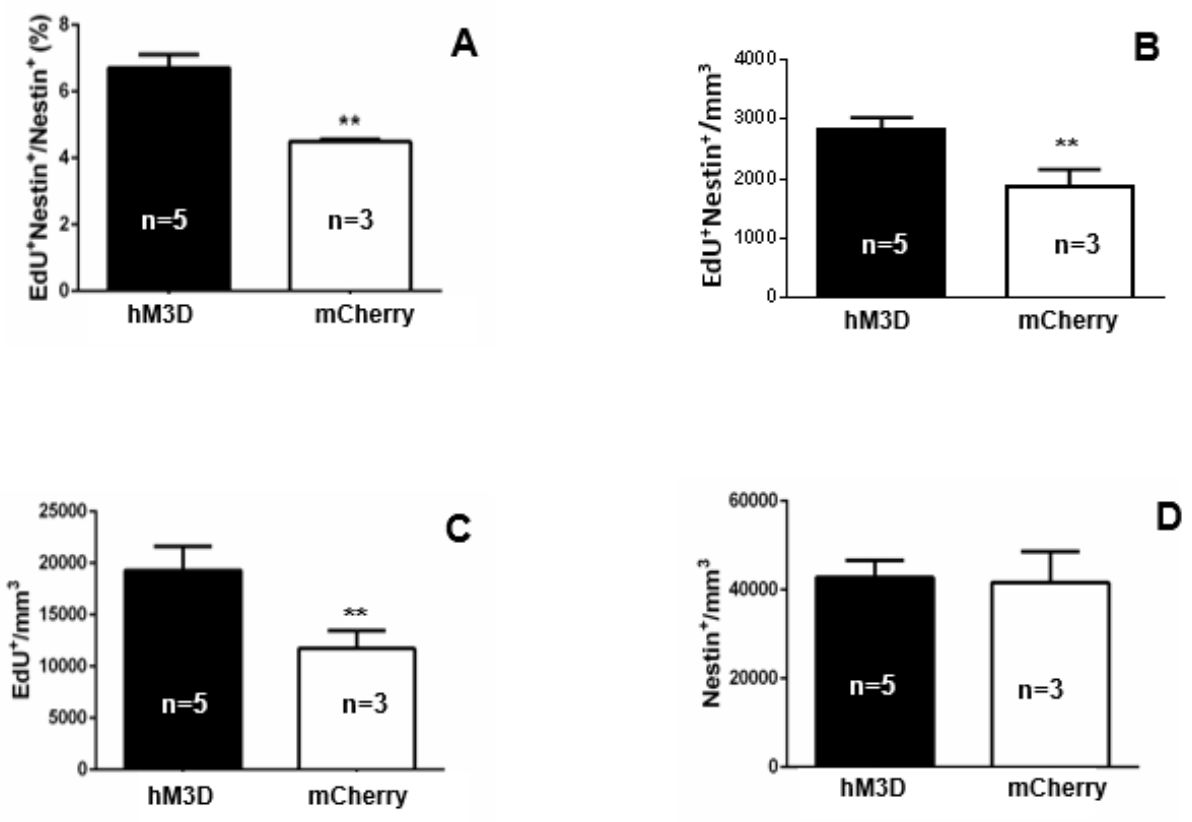

Figure 6. (A) DREADD activation of CCK-cells in the DG produced an increase in the percentage of proliferating NSCs (proliferating NSCs/total NSCs) in the DG. **(B)** CCK-cell stimulation increased the density of proliferating NSC (proliferating NSC/volume of DG). **(C)** CCK-stimulation increased total proliferation density in the DG (proliferating cells/volume of DG). **(D)** Activation of CCK-cells did not produce a significant increase in total NSC density (total NSCs/volume of DG). Error bars represent S.E.M., and ** denotes significance at $p < 0.05$.

3.5.1: Western blot

A western blot was performed to test the effectiveness of AAV-shRNA mediated knockdown of CCK8 (Figure 7A). The results indicated a 50% decrease in CCK8 concentration present in the cells compared to the scramble-shRNA (0.5193 ± 0.08697 vs. 1.075 ± 0.1211, $p=0.0204$; Figure 7B). In addition, the concentration of a control protein GAPDH was measured, and no reduction of protein concentration between the experimental and control groups was observed. These results indicated that knockdown of CCK8 was effective *in-vivo.*

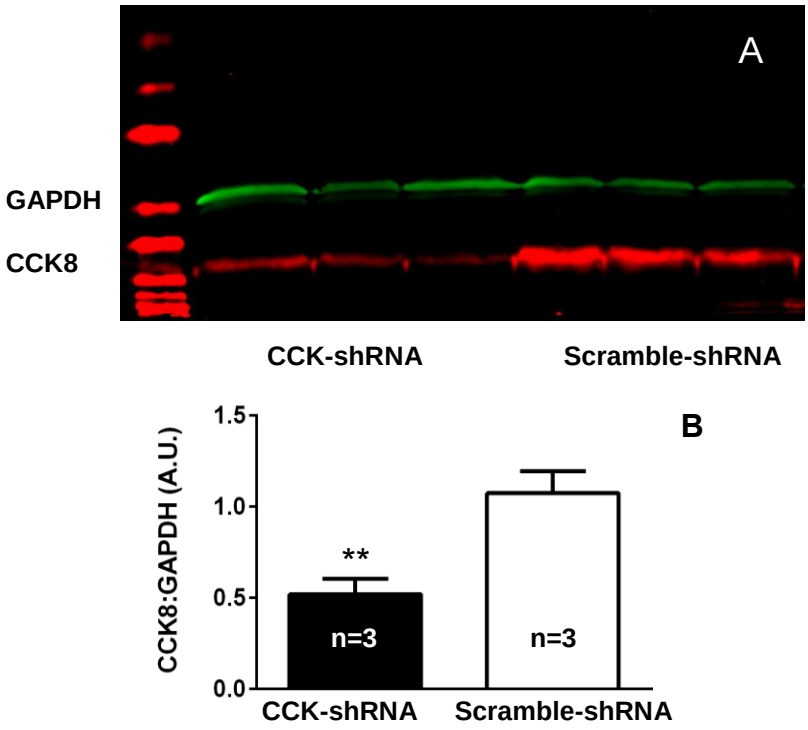

Figure 7. (A) Western blot revealing the effective knockdown of CCK8. **(B)** CCK-shRNA mediated 50% knockdown of CCK8. Error bars represent S.E.M., and ** denotes significance at $p < 0.05$.

3.5.2: Chemogenetic stimulation of CCK-cells following CCK8 knockdown

After the effectiveness of AAV-shRNA mediated knockdown of CCK8 was confirmed, the effects of CCK8 knockdown on NSC proliferation were investigated. Quantification of proliferating NSCs in the DG following knockdown and DREADD activation of CCK-cells revealed a significant reduction in the percentage of proliferating NSCs in comparison to the scramble-shRNA mice (2.356 ± 0.7147 vs. 5.767 ± 0.1965, p=0.0107; Figure 8A). Furthermore, in comparison to the scramble-shRNA mice, CCK8 knockdown significantly reduced both the density of proliferating NSCs (478.7 ± 113.8 vs. 1016 ± 90.16, p=0.0176; Figure 8B) and the total proliferation in the DG (5301 ± 747.5 vs. 9452 ± 1162, p=0.0251; Figure 8C) following CCK-cell activation. However, the decrease in proliferating NSCs did not translate to a significant change in total NSC density (21317 ± 1708 vs. 17345 ± 1410, p=0.1530; Figure 8D).

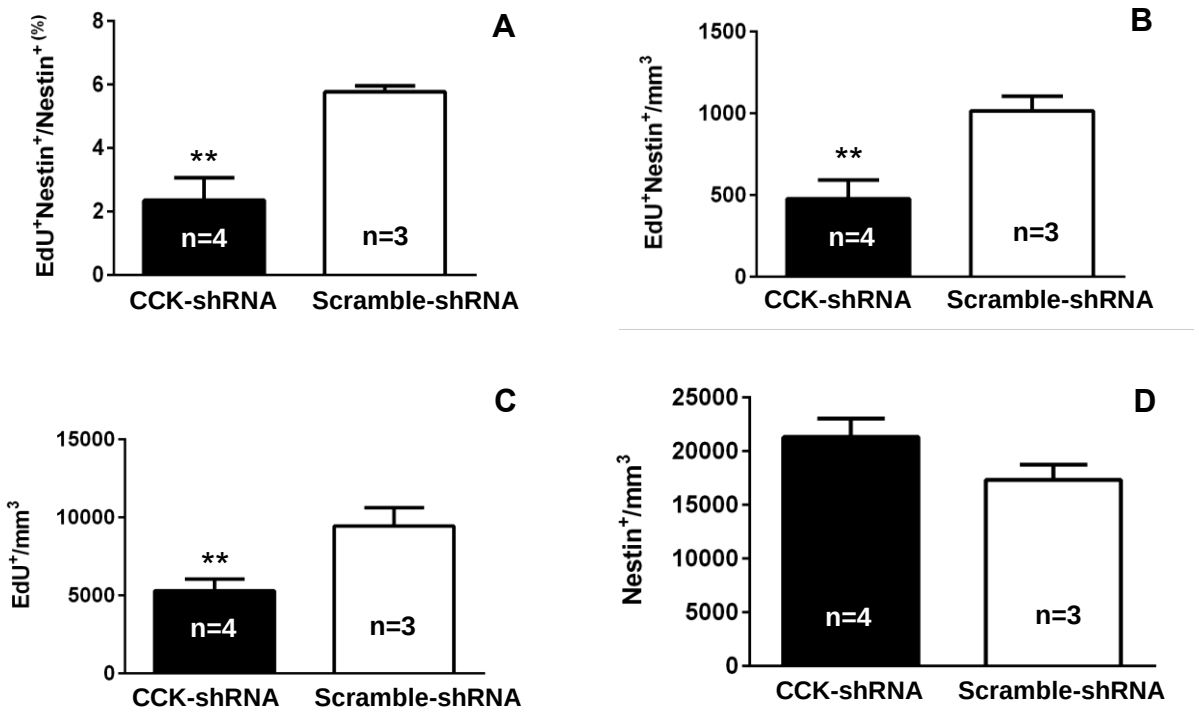

Figure 8. (A) shRNA-mediated knockdown of CCK8 reduced the percentage of proliferating NSCs (proliferating NSCs/total NSCs) following DREADD activation of CCK-cells in the DG. **(B)** CCK8 knockdown decreased the density of proliferating NSCs (proliferating NSC/volume of DG). **(C)** CCK8 knockdown reduced the total proliferation density in the DG (proliferating cells/volume of DG). **(D)** Knockdown of CCK8 did not produce a significant change in total NSC density (total NSCs/volume of DG). Error bars represent S.E.M., and ** denotes significance at $p<0.05$.

3.6: Chemogenetic activation of VGLUT3-expressing CCK-cells

CCK-cells exhibit heterogeneous attributes such as targeting different regions of the DG and expressing different subtypes[13]. One subset of CCK-cells expresses vesicular glutamate transporter 3 (VGLUT3), and densely innervates the SGZ[13]. Therefore, we investigated if selectively activating VGLUT3 CCK-cells was sufficient in recapitulating the observed effect of increasing NSC proliferation in the DG.

Similar to the results found in Section 3.4, DREADD-activation of VGLUT3 CCK-cells significantly increased the percentage of proliferating NSCs in comparison to the mice who received the AAV-DIO-mCherry injection and whose CCK-cells were not activated (6.986 ±

0.1455 vs. 4.958 ± 0.6373, p=0.0201; Figure 9A). However, unlike the results obtained in Section 3.4, there was no significant change seen in the total NSC proliferation density (1833 ± 269.5 vs. 1483 ± 192.8, p=0.3320; Figure 9B) or total proliferation density in the DG (30044 ± 5152 vs. 35545 ± 8182, p=0.5900; Figure 9C). No change in total NSC density in the DG was observed (26308 ± 4109 vs. 31111 ± 4347, p=0.4540; Figure 9D), which was similar to what we observed in Section 3.4.

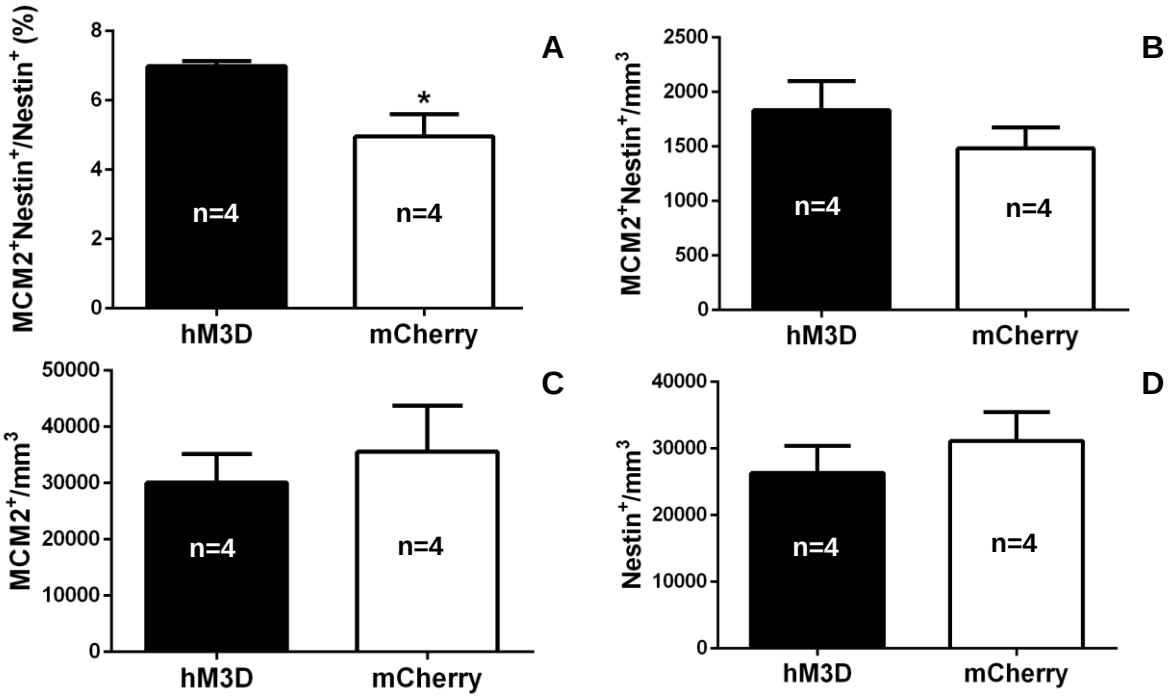

Figure 9. (A) DREADD activation of all VGLUT3 CCK-cells in the DG produced an increase in the percentage of proliferating NSCs (proliferating NSCs/total NSCs). **(B)** Activation of VGLUT3 CCK-cells did not produce a change in NSC proliferation density (proliferating NSC/volume of DG). **(C)** VGLUT3 CCK-cell activation did not produce a change in total proliferation density (proliferating cells/volume of DG). **(D)** DREADD activation did not produce a change in total NSC density (total NSCs/volume of DG). Error bars represent S.E.M., and * denotes significance at $p<0.05$.

4. Discussion

CCK, a neuropeptide expressed at high levels in the brain, has been implicated in regulating various physiological functions, including adult neurogenesis. Despite its relevance,

little is known about the intercellular mechanisms mediating CCK's function in this regulation. Therefore, the purpose of this ongoing study is to elucidate the role of the CCK-cell system in regulating adult neurogenesis. Preliminary results have indicated that CCK-cell projections are closely associated with NSCs. Therefore, we have proposed that CCK released from nearby synapses reaches CCK_2 receptors located on NSCs. We hypothesized that CCK functions to increase the proliferation of adult NSCs in the DG. To test this hypothesis, we used combinations of immunohistochemistry and chemogenetic tools to manipulate CCK activity *in-vivo*. DREADDs allowed *in-vivo* activation of CCK-cells without the risk of light-induced phototoxicity that often accompanies other methods such as optogenetics. As of yet, no similar study has taken a chemogenetic approach to study activity-dependent neurogenesis.

We have shown that NSCs possess CCK_2 receptors and that these receptors are likely to be functional. Chemogenetic activation of CCK-cells in two orthologous mouse lines increased the percentage of NSC proliferation. However, this effect did not translate to an increase in the total NSC population. shRNA-mediated knockdown of CCK8 was found to reduce the percentage of NSCs proliferating in the DG. This effect did not result in a decrease in the total NSC population.

4.1: NSCs likely express functional CCK_2 receptors

In-situ hybridization results indicated that NSCs expressed CCK_2 receptor mRNA. Furthermore, calcium-imaging data suggested that these receptors were likely functional as demonstrated by the significant increase in intracellular calcium release that followed the stimulation of these receptors by CCK8. This increase in intracellular calcium in NSCs was relayed as change in fluorescence. The observed calcium response was blocked after applying the CCK_2 receptor antagonist YM022, suggesting that the change in fluorescence was

induced by CCK8. Only one mouse was used in this calcium imaging experiment. Therefore, repeat experiments with larger sample sizes are necessary to ensure this effect is consistent among CCK_2 receptors in other CCK-Cre mice.

In addition to repeated calcium imaging experiments, patch clamp electrophysiology will be used to further study CCK_2 receptor activation. A drawback to calcium imaging is that there can be poor signal to noise ratios due to the use of chemical dyes. Additionally, indirect signals due to sodium influx during action potentials and synaptic activity can make calcium transients difficult to distinguish from background noise. Patch clamp recording will reduce some of those variables to retest CCK_2 receptor activity.

4.2: Chemogenetic activation of CCK-cells promotes the proliferation of NSCs

DREADD stimulation of CCK-cells in the DG produced a significant increase in both the percentage and density of NSC proliferation. The increase in percentage of proliferating NSCs following CCK-cell activation supports our hypothesis that CCK promotes the proliferation of NSCs. Proliferating NSC density measurements provided additional confirmation of this effect. Interestingly, we did not observe a change in the total density of NSCs following CCK-cell activation, but we did see a significant increase in the total density of proliferating cells in the DG. The lack of change in total NSC density suggests that CCK may stimulate NSCs to proliferate asymmetrically by differentiating instead of dividing into another NSC. The significant increase in total proliferating cell density also suggests that CCK may regulate other cells in the DG, such as neuroblasts or immature neurons, to differentiate or self-renew. Future studies will investigate later time points to study the role of CCK in cell differentiation and determining the fate-choice, survival, and integration of immature neurons into the surrounding neuronal circuitry.

4.3: Loss of CCK8 reduces NSC proliferation and total proliferation in the DG

Western blot analysis revealed that the AAV-expressing shRNA was successful at knocking down 50% of CCK8 synthesis. This loss in CCK8 resulted in a striking reduction of both the percentage and density of NSC proliferation after CCK-cell activation. These results thus show that knocking down CCK8 synthesis prevents the induction of NSC proliferation by CCK-cell activation. This further supports the role of CCK in promoting NSC proliferation. In addition, we did not observe a change in the total NSC density, but we did see a significant decrease in the total proliferating cell density in the DG. The data also provide further support that CCK may promote the asymmetrical proliferation of NSCs and play a role in regulating the proliferation of other cell types in the DG. Since CCK-cells can release several molecular forms of CCK that have affinity to the CCK_2 receptor[8,9], future studies will investigate whether knocking down other forms of CCK is sufficient in recapitulating this effect of reducing NSC proliferation. This will help determine whether or not this effect is specific to CCK8.

4.4: Chemogenetic activation of VGLUT3 CCK-cells promotes the proliferation of NSCs

Due to the fact that a heterogeneous population of cells releases CCK, we sought to identify the specific components of the CCK-cell system to better understand how this system may be involved in adult neurogenesis. Previous studies have indicated that a subset of CCK-cells express VGLUT3[13,20]. Therefore, we proposed that VGLUT3 CCK-cells were potential candidates in producing the observed effect of CCK on NSC proliferation.

Results showed that similar to DREADD activation of all CCK-cells in the DG, activation of VGLUT3 CCK-cells produced the same effect of significantly increasing the percentage of NSC proliferation. This indicated that activation of the VGLUT3-expressing subpopulation of CCK-cells was sufficient in producing an increase in NSC proliferation—

providing support for our central hypothesis. While we did not observe an increase in the density of proliferating NSCs, this experiment was a secondary measure and may reflect the reduced number of CCK-cells recruited in this experiment. Since VGLUT3 CCK-cells represent a subset of the entire CCK-cell population, activation of VGLUT3 CCK-cells for this short duration may not have been sufficient to fully expand this proliferating population to the point of a significant difference.

4.5: Future directions

In summary, these data strengthen the implication of CCK as being a positive regulator of adult neurogenesis. We will continue examining the significance of these findings using behavioral assays to observe the importance of this system in specific neurogenesis-associated tasks. In addition, later time-points of adult hippocampal neurogenesis will be investigated to probe the role of CCK in regulating cell-differentiation and fate-choice, survival, and dendritic and synaptic integration. This information could potentially contribute to future treatment programs for neurodegenerative diseases by utilizing CCK-receptor agonists or antagonists and facilitating the regeneration of neurons after brain injury. Understanding the role of local signaling in promoting proliferation, survival, and integration of newborn neurons into existing neural circuitry is necessary for the future of such promising therapies.

5. Acknowledgments

First and foremost, I would like to thank my graduate student mentor and co-investigator, Reid Olsen, for his assistance and unwavering support during the past three years. Reid collected the calcium imaging and CCK-cell activation data (Sections 3.3 and 3.4). For these parts, I only assisted in performing the experiments. Thank you to Dr. Alison Xie for her help with the calcium imaging. The CCK and CCK8 antibodies were generous gifts from Dr. Margery

Beinfeld at Tufts University and Dr. Andrea Varro at Liverpool University, respectively. Lastly, I would like to express my gratitude to Dr. Juan Song and all of the members of the Song Lab for facilitating such a positive learning environment for me in the lab.

This research is supported by Reid's NRSA, the Summer Undergraduate Research Fellowship from the Office of Undergraduate Research at UNC, and the Taylor Honors Fellowship sponsored by Honors Carolina and William W. and Ida W. Taylor.

6. References

1. Cajal, Santiago Ramón. *Degeneration & regeneration of the nervous system*. Vol. 1. Oxford University Press, Humphrey Milford, **1928**.
2. Ge, Shaoyu, Dennis A. Pradhan, Guo-li Ming, and Hongjun Song. "GABA sets the tempo for activity-dependent adult neurogenesis." *Trends in neurosciences* 30, no. 1 **(2007)**: 1-8.
3. Ming, Guo-li, and Hongjun Song. "Adult neurogenesis in the mammalian central nervous system." *Annu. Rev. Neurosci.* 28 **(2005)**: 223-250.
4. Bordey, Angélique. "Adult neurogenesis: basic concepts of signaling." *Cell Cycle* 5, no. 7 **(2006)**: 722-728.
5. Spalding, Kirsty L., Olaf Bergmann, Kanar Alkass, Samuel Bernard, Mehran Salehpour, Hagen B. Huttner, Emil Boström et al. "Dynamics of hippocampal neurogenesis in adult humans." *Cell* 153, no. 6 **(2013)**: 1219-1227.
6. Ming, Guo-li, and Hongjun Song. "Adult neurogenesis in the mammalian brain: significant answers and significant questions." *Neuron* 70, no. 4 **(2011)**: 687-702.
7. Song, Juan, Chun Zhong, Michael A. Bonaguidi, Gerald J. Sun, Derek Hsu, Yan Gu, Konstantinos Meletis et al. "Neuronal circuitry mechanism regulating adult quiescent neural stem-cell fate decision." *Nature* 489, no. 7414 **(2012)**: 150-154.
8. Langmesser, Sonja, Maria I. Cerezo-Guisado, Maria J. Lorenzo, Luis J. Garcia-Marin, and Maria J. Bragado. "CCK1 and 2 receptors are expressed in immortalized rat brain neuroblasts: intracellular signals after cholecystokinin stimulation." *Journal of cellular biochemistry* 100, no. 4 **(2007)**: 851-864.
9. Daugé, Valérie, Angélique Sebret, Françoise Beslot, Toshimitsu Matsui, and Bernard P. Roques. "Behavioral profile of CCK2 receptor-deficient mice."*Neuropsychopharmacology* 25, no. 5 **(2001)**: 690-698.
10. Greenstein, R. J., M. M. Ybanez, R-L. Zhang, and W. A. Bauman. "Is aging preprogrammed? Observations from the brain/gut axis." *Mechanisms of ageing and development* 61, no. 2 **(1991)**: 113-121.
11. Harro, Jaanus, and Lars Oreland. "Age-related differences of cholecystokinin receptor binding in the rat brain." *Progress in Neuro-Psychopharmacology and Biological Psychiatry* 16, no. 3 **(1992)**: 369-375.
12. Stanić, Davor, Gustavo Paratcha, Fernanda Ledda, Herbert Herzog, Alan S. Kopin, and Tomas Hökfelt. "Peptidergic influences on proliferation, migration, and placement of

neural progenitors in the adult mouse forebrain." *Proceedings of the National Academy of Sciences* 105, no. 9 **(2008)**: 3610-3615.
13. Somogyi, Jozsef, Agnes Baude, Yuko Omori, Hidemi Shimizu, Salah El Mestikawy, Masahiro Fukaya, Ryuichi Shigemoto, Masahiko Watanabe, and Peter Somogyi. "GABAergic basket cells expressing cholecystokinin contain vesicular glutamate transporter type 3 (VGLUT3) in their synaptic terminals in hippocampus and isocortex of the rat." *European Journal of Neuroscience*19, no. 3 **(2004)**: 552-569.
14. Menon, Shalini, Nicholas Patrick Boyer, Cortney Chelise Winkle, Leslie Marie McClain, Christopher Carey Hanlin, Dharmendra Pandey, Simon Rothenfußer, Anne Marion Taylor, and Stephanie Lynn Gupton. "The E3 Ubiquitin Ligase TRIM9 Is a Filopodia Off Switch Required for Netrin-Dependent Axon Guidance." *Developmental cell* 35, no. 6 **(2015)**: 698-712.
15. Stuber, Garret D., Alice M. Stamatakis, and Pranish A. Kantak. "Considerations when using cre-driver rodent lines for studying ventral tegmental area circuitry." *Neuron* 85, no. 2 **(2015)**: 439-445.
16. Xie, Alison X., Kelli Lauderdale, Thomas Murphy, Timothy L. Myers, and Todd A. Fiacco. "Inducing plasticity of astrocytic receptors by manipulation of neuronal firing rates." *Journal of visualized experiments: JoVE* 85 **(2014)**.
17. Arey, Rachel N., J. F. Enwright, Sade M. Spencer, Edgardo Falcon, Angela R. Ozburn, Subroto Ghose, Carol Tamminga, and Colleen A. McClung. "An important role for Cholecystokinin, a CLOCK target gene, in the development and treatment of manic-like behaviors." *Molecular psychiatry* 19, no. 3 **(2014)**: 342-350.
18. Bonaguidi, Michael A., Michael A. Wheeler, Jason S. Shapiro, Ryan P. Stadel, Gerald J. Sun, Guo-li Ming, and Hongjun Song. "In vivo clonal analysis reveals self-renewing and multipotent adult neural stem cell characteristics." *Cell* 145, no. 7 (2011): 1142-1155.Jao, Cindy Y., and Adrian Salic. "Exploring RNA transcription and turnover in vivo by using click chemistry." *Proceedings of the National Academy of Sciences* 105, no. 41 **(2008)**: 15779-15784.
19. Salic, Adrian, and Timothy J. Mitchison. "A chemical method for fast and sensitive detection of DNA synthesis in vivo." *Proceedings of the National Academy of Sciences* 105, no. 7 **(2008)**: 2415-2420.
20. Fremeau, Robert T., Jonathon Burman, Tayyaba Qureshi, Cindy H. Tran, John Proctor, Juliette Johnson, Hui Zhang et al. "The identification of vesicular glutamate transporter 3 suggests novel modes of signaling by glutamate." *Proceedings of the National Academy of Sciences* 99, no. 22 **(2002)**: 14488-14493.